

Shear-Induced Crystallization of Injection Molded Vetiver Grass-Polypropylene Composites

Usa Somnuk,^{1,2} Nitinat Suppakarn,^{1,2} Wimonlak Sutapun,^{1,2} Yupaporn Ruksakulpiwat^{1,2}

¹School of Polymer Engineering, Institute of Engineering, Suranaree University of Technology, Nakhon Ratchasima 30000, Thailand

²Center of Excellent for Petroleum, Petrochemical and Advanced materials, Chulalongkorn University, Bangkok 10330, Thailand

Received 13 November 2007; accepted 22 March 2009

DOI 10.1002/app.30459

Published online 27 May 2009 in Wiley InterScience (www.interscience.wiley.com).

ABSTRACT: Vetiver grass was used as an alternative filler in polypropylene (PP) composites in this study. Chemical treatment of vetiver grass by alkalization was carried out to obtain alkali-treated vetiver grass. It was shown that alkali-treated vetiver grass exhibited higher thermal stability than untreated vetiver grass. Injection molding was used to prepare the composites. The microstructure of injection molded samples showed a distinct skin layer due to shear-induced crystallization. It was found that normalized thickness of shear-induced crystallization layer of the composite was lower than that of neat PP. The effect of vetiver particle sizes on shear-induced crystallization and physical properties of the composites were elucidated. Furthermore, the effect of processing conditions on shear-

induced crystallization, degree of crystallinity, gapwise crystallinity distribution, and mechanical properties of the composite were investigated. It was shown that injection speed and mold temperature affected the normalized thickness of shear-induced crystallization layer and degree of crystallinity of the composites. However, processing conditions showed insignificant effect on the mechanical properties of vetiver fiber-PP composites. The degree of crystallinity showed no distribution throughout the thickness direction of the composites. © 2009 Wiley Periodicals, Inc. *J Appl Polym Sci* 113: 4003–4014, 2009

Key words: crystallization; mechanical properties; microstructure; injection molding; composites

INTRODUCTION

Natural fibers, such as kenaf, coir, flax, and jute can be potentially served as inexpensive fillers for polymers. The advantages of natural fibers over synthetic fibers are low cost, low-specific density, and low abrasive wear during processing. Furthermore, the natural fibers are abundant, biodegradable, and renewable.¹ According to His Majesty the King Bhumibol Adulyadej of Thailand's Royal Initiative, the main purpose of vetiver grass cultivation is to conserve soil and water resources, particularly for the steep slope areas. Normally, leaves of vetiver grass have been cut every few months to keep the vetiver rows in order. Only a minor portion of the residues is reserved as animal feed or household fuel. On the other hand, huge quantities of the remaining residues are burnt in fields or on the side of road.^{2,3} Therefore, using such a residue as a filler in polymer

composites are challenging approaches. From our previous study,⁴ it was found that vetiver grass-polypropylene (PP) composite, compared with neat PP, exhibited higher tensile strength and Young's modulus but lower elongation at break and impact strength. This implied that vetiver grass could be served as a reinforcing filler in PP composites.

Injection molding is one of the most important processing operations widely used to produce products from natural fiber-PP composites because the products can be easily formed into complex shapes and can be produced as mass productions. The processing conditions of the injection molding can have the effect on the crystallization and morphology of the products. Hence, they govern the physical and mechanical properties of the molded parts. During injection molding, plastics undergo fountain flow. The molten polymer is subjected to high shear stress at the cavity wall which causes the preferential orientation of the molecular chains. As a result, a skin layer or shear-induced crystallization layer with a high molecular orientation takes place at the surface of moldings. On the other hand, in the core of moldings, the relaxation of the molecular chain occurs due to the low cooling rates and low shear stress so the effect of shear on crystallization can be neglected. As a result, at the core region quiescent crystallization takes place. The spherulites

Correspondence to: Y. Ruksakulpiwat (yupa@sut.ac.th).

Contract grant sponsor: Thailand Research Fund, Suranaree University of Technology and Center of Excellent for Petroleum, Petrochemical and Advanced materials, Chulalongkorn University.

with very low molecular orientation can be observed at the core. Quiescent crystallization of PP composites from natural fibers was investigated in our previous study.⁵ Understanding the crystallization occurred in the injection molded samples is highly important because it relates the morphology and also the properties of products. Particularly, the mechanical properties of injection molded samples are determined to some extent by shear-induced crystallization and microstructure developed on processing. Although the shear-induced crystallization of PP has already been well understood,⁶ the shear-induced crystallization of PP composites, has not been studied so far.

Hence, this study was intended to characterize the vetiver grass by means of thermal, functional, and morphological analysis. The effect of vetiver particle sizes on rheological, thermal, and mechanical properties of PP composites was examined. The effect of vetiver particle sizes on shear-induced crystallization of PP composites was explored as well. Moreover, the effect of processing conditions on shear-induced crystallization, degree of crystallinity, gapwise crystallinity distribution, and mechanical properties of PP composites were investigated.

EXPERIMENTAL PROCEDURES

Materials

A commercial grade of isotactic PP (700J) was supplied by Thai Polypropylene Co., Ltd. (Thailand). Vetiver grass (*Vetiveria zizanioides*) was obtained from The Land Development Department, Nakhon Ratchasima, Thailand. In this research, vetiver leaves with length of 30 cm from vetiver culm were used. The ages of vetiver grass are ~6–8 months. Sodium hydroxide (NaOH), laboratory grade, purchased from Merck Co., Inc. (Thailand) was used.

Sample preparations and characterization

Alkali-treated vetiver grass preparation and characterization

Vetiver grass was washed by water to eliminate dirt and dried in an oven at 100°C for 24 h. Vetiver grass before alkalization was called untreated vetiver grass. Alkalization was performed by immersing vetiver grass in 4% (wt) NaOH solution for 2 h at 40°C. Vetiver grass obtained after alkalization process was called alkali-treated vetiver grass. The thermogravimetric analysis of untreated and alkali-treated vetiver grass was done by heating the samples from 30 to 800°C at a heating rate of 20°C/min under a nitrogen atmosphere using TGA model SDT 2960. DRIFT spectra of untreated and alkali-treated vetiver grass were recorded by a Perkin-Elmer FTIR spectrometer (model Spectrum GX: FTIR).

TABLE I
Processing Conditions for Injection Molding of Vetiver Fiber-PP Composites

Processing condition	Screw speed (rpm)	Injection speed (mm/s)	Holding pressure (kg/cm ²)	Mold temperature (°C)
1	130	46	1400	25
2	65	46	1400	25
3	195	46	1400	25
4	130	18.4	1400	25
5	130	82.8	1400	25
6	130	18.4	1400	45
7	130	18.4	1400	65
8	130	46	840	25
9	130	46	2240	25

Vetiver fiber-PP and vetiver powder-PP composite preparation and characterization

After the alkalization process, the alkali treated vetiver grass was prepared into two forms: (a) vetiver fiber, with 2 mm in length and (b) vetiver powder, which its mean particle size was 57.48 μm. To prepare vetiver fiber-PP composite, vetiver fiber was mixed with PP using an internal mixer (Haake Rheomix 3000P model 557-1306) at 170°C. The ratio of vetiver fiber to PP was fixed at 20 : 80 by weight. This mixing procedure was also applied to mix vetiver powder to PP to obtain vetiver powder-PP composite. After that, vetiver fiber-PP and vetiver powder-PP composite were ground and dried before molding.

Shear viscosities at the shear rate range of 10–10,000 s⁻¹ of neat PP, vetiver fiber-PP, and vetiver powder-PP composites were measured using Kayeness capillary rheometer at 180°C.

Injection molded specimens preparation and characterization

Neat PP, vetiver fiber-PP, and vetiver powder-PP composite were molded by injection molding (Chuan Lih Fa Machine model CLF-80T). Processing conditions including screw speed, injection speed, holding pressure, and mold temperature were varied as summarized in Table I. Processing conditions 1, 2, and 3 were used to study the effect of screw speed on shear-induced crystallization and mechanical properties of the composites. Processing conditions 1, 4, and 5 were used to examine the effect of injection speed on shear-induced crystallization and mechanical properties of the composites. Processing conditions 1, 8, and 9 were used to elucidate the effect of holding pressure on shear-induced crystallization and mechanical properties of the composites. In addition, processing conditions 4, 6, and 7 were used to investigate the effect of mold temperature on shear-induced crystallization and mechanical properties of the composites.

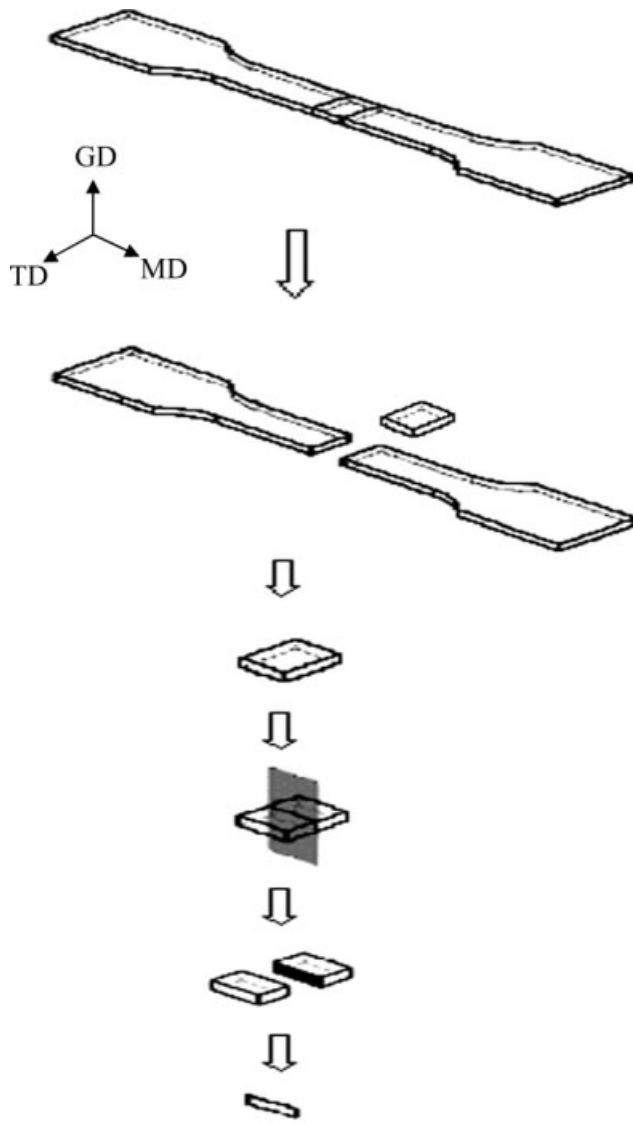


Figure 1 Sample cutting procedure to study the shear-induced crystallization layer.

The injection molded specimens were cut perpendicular to machine direction (MD) and parallel to transverse direction at the center of the specimens. Subsequently, the specimen was cut throughout the center plane and parallel to MD using Rotary Microtome (RMC model MT 960) into a thin film of 50 μm thickness. The cutting procedure was illustrated in Figure 1. The morphology of the specimens was investigated using a Polarized Light Optical Microscope (Nikon: model Eclipses E600 POL). Normalized thickness of shear-induced crystallization layer was determined using the following equation.

$$\text{Normalized thickness of shear-induced crystallization layer (\%)} = \frac{\text{Skin layer thickness}}{\text{Total thickness of test specimen}} \times 100 \quad (1)$$

Degree of crystallinity (% crystallinity) of injection molded samples at various depths was determined by differential scanning calorimetry (DSC: Mettler Toledo Version STAR^e SW 8.1). Composite samples at various depths (Y) in the thickness direction (H) were obtained by cutting the samples with Rotary Microtome into a thin film of 50 μm thickness (Fig. 2). The depth of the sample was varied into four zones, which were referred to different Y/H value. The Y/H value was ranged from 0 to 1. In a case of $Y/H = 1$, it is referred to the skin of the sample. Whereas $Y/H = 0$ is referred to the core (center) of the sample. The weight of each specimen was

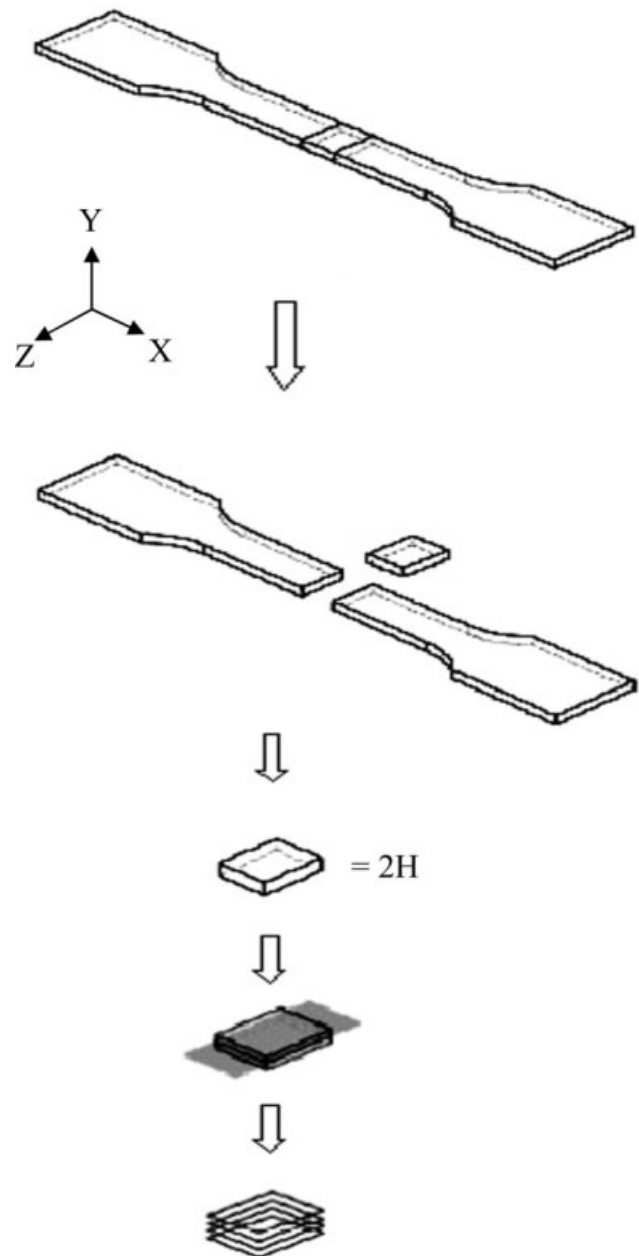


Figure 2 Sample cutting procedure to study the degree of crystallinity.

~ 5 mg. To measure the degree of crystallinity of the sample, the sample was heated from 25°C to 200°C with a heating rate of 10°C/min. The degree of crystallinity (X_c) was determined using the following equation.⁷

$$X_c(\% \text{crystallinity}) = \frac{\Delta H_f}{\Delta H_f^\circ W} \times 100 \quad (2)$$

where ΔH_f is a latent heat of fusion of a sample (area under the melting peak), ΔH_f° is the latent heat of fusion of a 100% crystalline PP (207.1 J/g⁸), and W is the weight fraction of PP in the composite.

Tensile testing was performed according to ASTM D638 using an Instron Universal Testing Machine (model 5569), at a crosshead speed of 10 mm/min and a gauge length of 80 mm. Impact tests were performed according to ASTM D256 using an impact tester (basic pendulum tester, Atlas model BPI).

RESULTS AND DISCUSSION

Characterization of alkali-treated vetiver grass

TGA and DTG curves of untreated vetiver grass, and alkali-treated vetiver grass are displayed in Figure 3. The TGA curve of each sample showed an initial transition around 100°C due to moisture evaporation. The DTG curve of untreated vetiver grass showed the second decomposition peak around 333°C. This peak was an integral peak derived from the decomposition of both hemicellulose and α -cellulose components. However, the decomposition of hemicellulose was observed in the DTG curve of alkali-treated vetiver grass as a shoulder peak around 310°C. In addition, the decomposition of α -cellulose was clearly observed at 365°C in the DTG curve of alkali-treated vetiver grass. The decomposition temperatures of hemicellulose and α -cellulose of vetiver grass were in the same range as those of jute, hemp, and sisal.^{9–11} Moreover, TGA curve of the alkali-treated vetiver grass exhibited higher onset decomposition temperature (320°C) than that of the untreated vetiver grass (275°C). This indicated that the alkali-treated vetiver grass has higher thermal resistance than the untreated vetiver grass. This might be due to the removal of some components degraded at lower temperature, such as lignin, pectin, hemicellulose, and waxy substances from the vetiver grass.

Diffuse reflection infrared Fourier transform (DRIFT) spectra of untreated and alkali-treated vetiver grass are shown in Figure 4. Significant changes of DRIFT spectra were observed from three peaks at 1734, 899, and 832 cm⁻¹, respectively. The peak at 1734 cm⁻¹ is due to the C=O stretching of hemicellulose. The intensity of this peak was considerably reduced for the alkali-treated vetiver grass

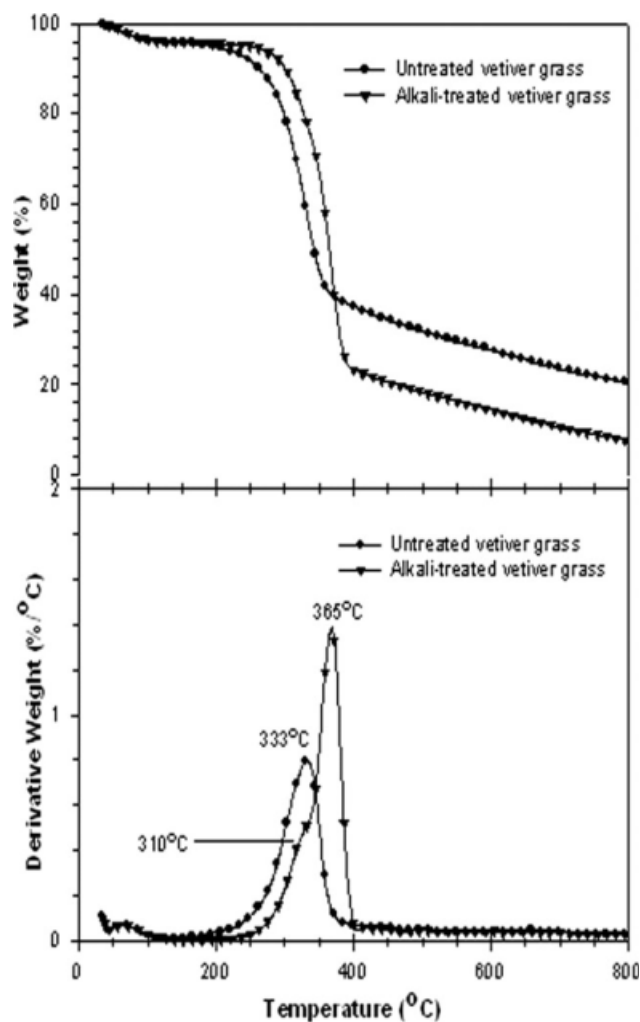


Figure 3 TGA and DTG curves of untreated vetiver grass and alkali-treated vetiver grass.

indicating the removal of the hemicellulose by the alkali treatment. Other two peaks at 899 and 832 cm⁻¹ are due to the O—C—O stretching in β -glucosidic linkage.^{12,13} However, the peak at 832 cm⁻¹ disappeared in case of the alkali-treated vetiver grass. This confirmed that NaOH solution can remove hemicellulose from vetiver grass. Other studies reported that during alkalization of plant fibers, the fine structure of cellulose may have been changed from the native cellulose I to cellulose II within the crystalline domain of the fiber cellulose. However, the extent of polymorphic transformation of cellulose I into cellulose II was dependent on NaOH concentration.^{14,15}

SEM micrographs of untreated vetiver grass and alkali-treated vetiver grass are represented in Figure 5. SEM micrograph of alkali-treated vetiver grass revealed fibrils with a rough surface topography. This may be due to the leach out of alkali-soluble fractions like waxy layer, lignin, and hemicellulose,

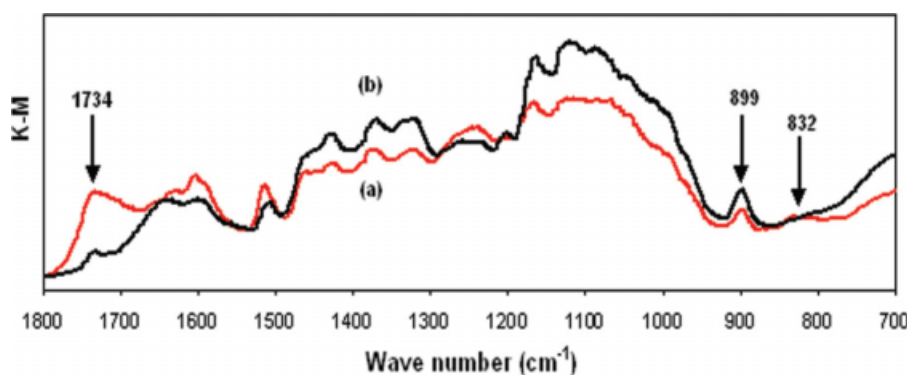


Figure 4 DRIFT Spectra of (a) untreated vetiver grass and (b) alkali-treated vetiver grass. [Color figure can be viewed in the online issue, which is available at www.interscience.wiley.com.]

which was confirmed by DRIFT spectra and TGA curve as previously mentioned. An increase in the surface roughness of the fiber after alkalinization is expected to result in a better mechanical interlocking. Also an increase in amount of exposed cellulose on the fiber surface would lead to an increase in the number of possible reaction sites. So the alkali-treated vetiver grass in the form of vetiver fiber and vetiver powder are used to prepare the vetiver fiber-PP and vetiver powder-PP composites, respectively.

The effect of vetiver particle sizes on PP composites

Rheological property

Shear viscosities of both vetiver fiber-PP and vetiver powder-PP composites were higher than that of neat PP as shown in Figure 6. This was possibly because vetiver particles perturbed normal flow of PP and hindered the mobility of chain segments in the melt flow. In addition, viscosity of vetiver fiber-PP composites was slightly higher than that of vetiver

powder-PP composites. This suggested that the larger particle of vetiver grass was able to obstruct normal flow of polymer and impede the mobility of chain segments in the flow more than the smaller particle of vetiver grass.

Thermal property

TGA and DTG thermograms of neat PP, vetiver fiber, vetiver powder, vetiver fiber-PP composites and vetiver powder-PP composites are shown in Figure 7. It can be observed that both vetiver fiber-PP and vetiver powder-PP composites showed the similar TGA and DTG patterns. Moreover, the thermograms revealed that the onset of the decomposition temperature of vetiver fiber-PP and vetiver powder-PP composites was lower than that of neat PP (Fig. 7). This was due to the lower thermal stability of vetiver fiber and vetiver powder in comparison with that of neat PP. Vetiver fiber-PP and vetiver powder-PP composites showed the first decomposition peak at $\sim 365^{\circ}\text{C}$ due to α -cellulose decomposition of

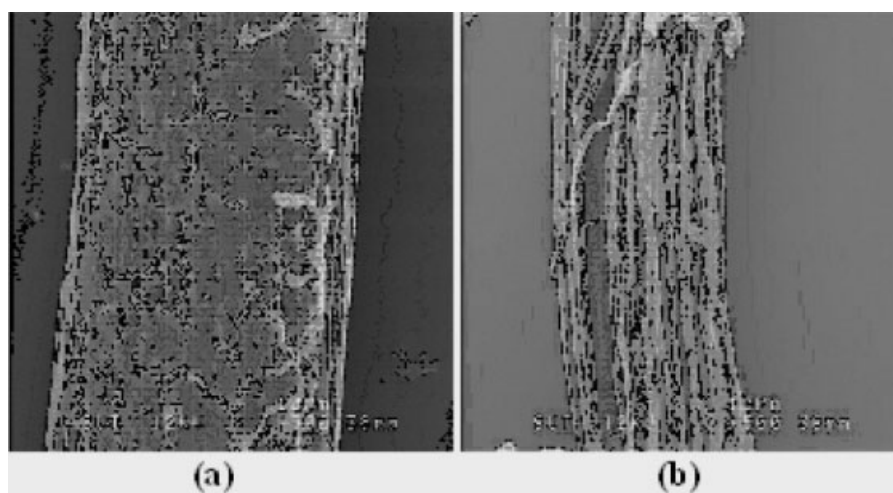


Figure 5 SEM micrographs of (a) untreated vetiver grass and (b) alkali-treated vetiver grass.

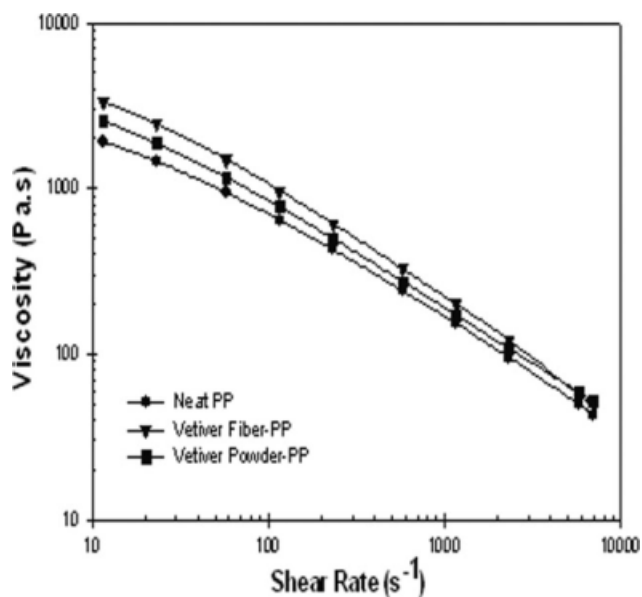


Figure 6 Flow curves of neat PP, vetiver fiber-PP, and vetiver powder-PP composites.

vetiver grass.⁴ The second decomposition peak at $\sim 460^\circ\text{C}$ indicated the degradation of saturated and unsaturated carbon atoms in PP.¹¹

Mechanical properties

Mechanical properties of neat PP and PP composites are shown in Table II. Both vetiver fiber-PP and vetiver powder-PP composites exhibited higher tensile strength and Young's modulus than those of neat PP. This is because the tensile strength and Young's modulus of vetiver fiber are much higher than that of neat PP. The tensile strength and Young's modulus of vetiver fiber used in this study were in the range of 247–723 MPa and 12.0–49.8, respectively.⁴ According to Table II, elongation at break and impact strength of both vetiver fiber-PP composites and vetiver powder-PP composites were lower than that of neat PP. This is because an introduction of vetiver fiber or vetiver powder into PP matrix results in a heterogeneous system, which induces stress concentration from external loading. Heterogeneous stress distribution developing in the composites obviously affects its deformation and failure behavior.¹⁶ It is widely accepted that fillers

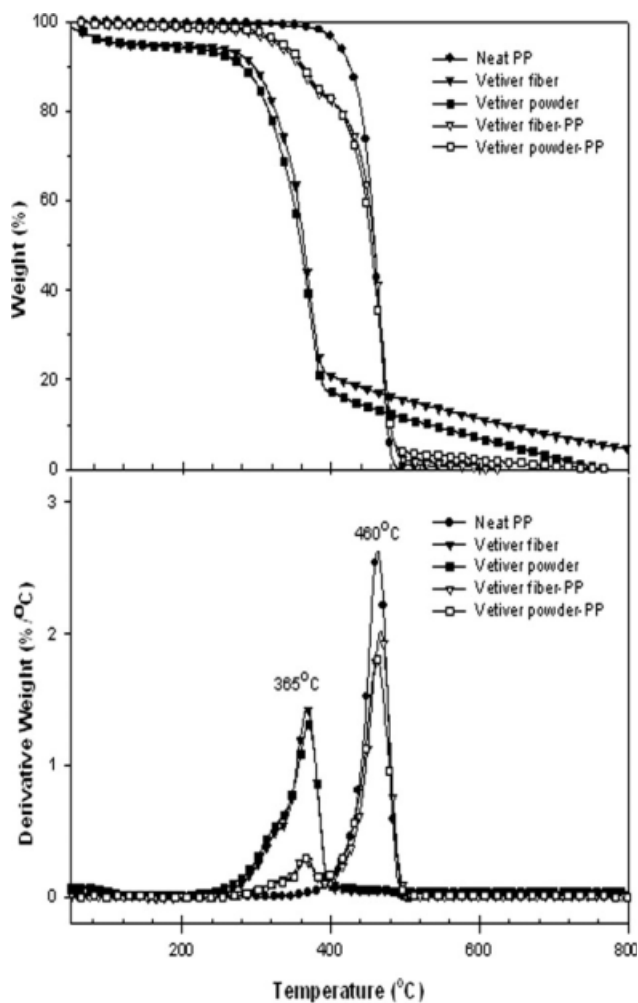


Figure 7 TGA and DTG curves of neat PP, vetiver fiber, vetiver powder, vetiver fiber-PP, and vetiver powder-PP composites.

enhance the stiffness by sacrificing the ductility (yield and elongation behavior) and toughness performance of the matrix polymer, resulting in an apparently brittle material.¹⁷

In addition, vetiver fiber-PP composites showed slightly higher tensile strength and Young's modulus than vetiver powder-PP composites. This was possibly because vetiver fiber was able to transfer load applied to composites more than vetiver powder. The strength of fiber-reinforced composites depends not only on the tensile strength of the fiber,

TABLE II
Mechanical Properties of Neat PP, Vetiver Fiber-PP, and Vetiver Powder-PP Composites

Designation	Impact strength (kJ/m ²)	Tensile strength (MPa)	Young's modulus (GPa)	Elongation at break (%)
Neat PP	69.69 ± 2.09	13.68 ± 1.74	1.13 ± 0.03	143.55 ± 19.67
Vetiver fiber-PP	18.91 ± 1.25	26.48 ± 0.54	1.43 ± 0.04	8.36 ± 0.57
Vetiver powder-PP	19.12 ± 0.70	22.09 ± 0.63	1.26 ± 0.08	11.84 ± 3.00

TABLE III
Normalized Thickness of Shear-Induced Crystallization Layer of Neat PP, Vetiver Fiber-PP and Vetiver Powder-PP Composites

Designation	Normalized thickness of shear-induced crystallization layer (%)
Neat PP	8.22
Vetiver fiber-PP	6.87
Vetiver powder-PP	7.33

but also on the degree to which an applied load is transmitted to the fibers. It was known that the extent of load transmittance is a function of fiber length and the magnitude of the fiber-matrix interfacial bond.¹⁸ However, the elongation at break and

the impact strength of both vetiver fiber-PP and vetiver powder-PP showed insignificant difference.

Normalized thickness of shear-induced crystallization layer

Table III shows the normalized thickness of shear-induced crystallization layer of neat PP, vetiver fiber-PP, and vetiver powder-PP composites. It was observed that normalized thickness of shear-induced crystallization layer of neat PP was higher than those of vetiver fiber-PP and vetiver powder-PP composites. In addition, vetiver fiber-PP composite exhibited lower normalized thickness of shear-induced crystallization layer than vetiver powder-PP composite. This is because the larger vetiver

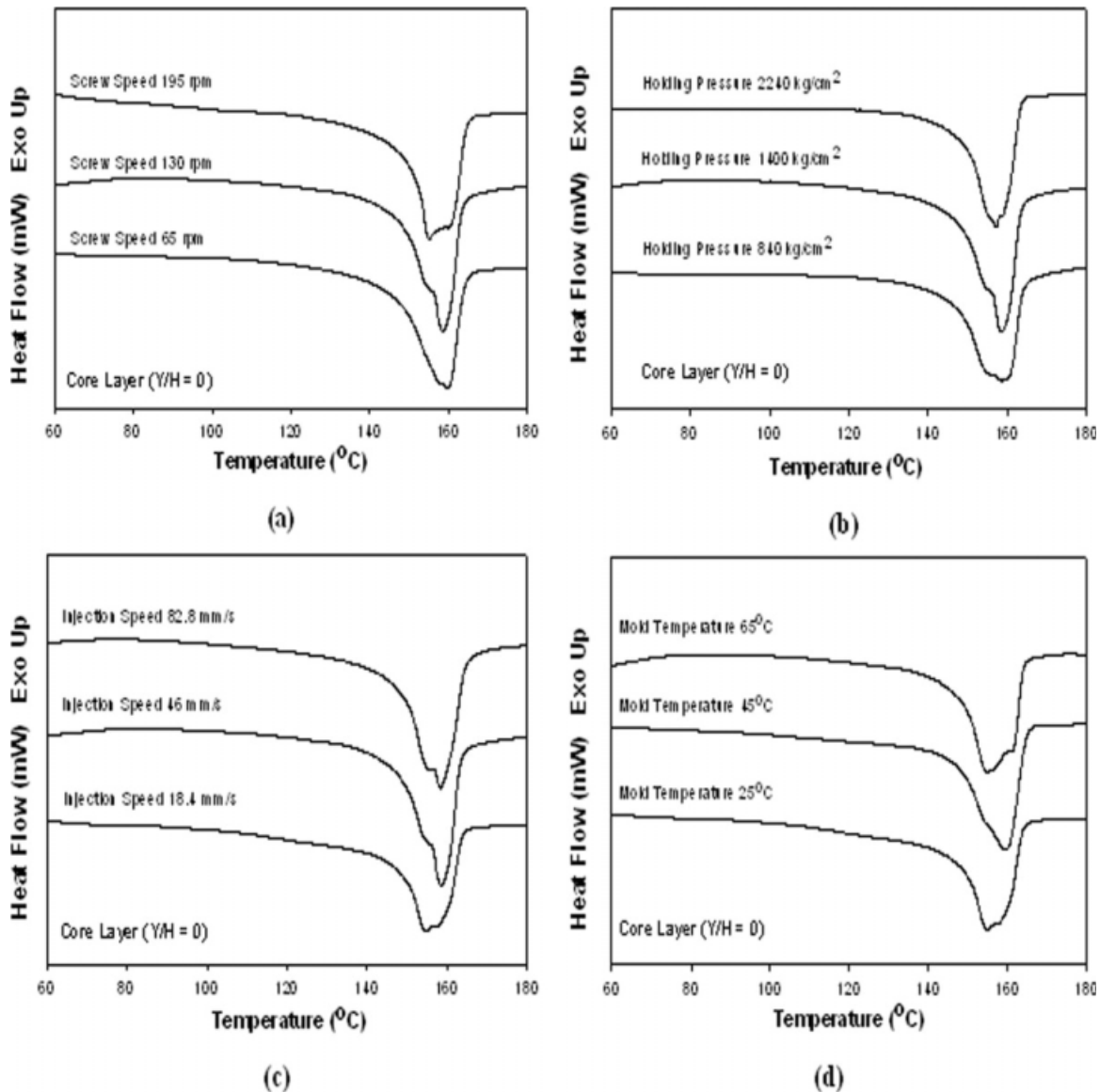


Figure 8 DSC curves of vetiver fiber-PP composites at core layer ($Y/H = 0$) at various (a) screw speeds, (b) holding pressures, (c) injection speeds, and (d) mold temperatures.

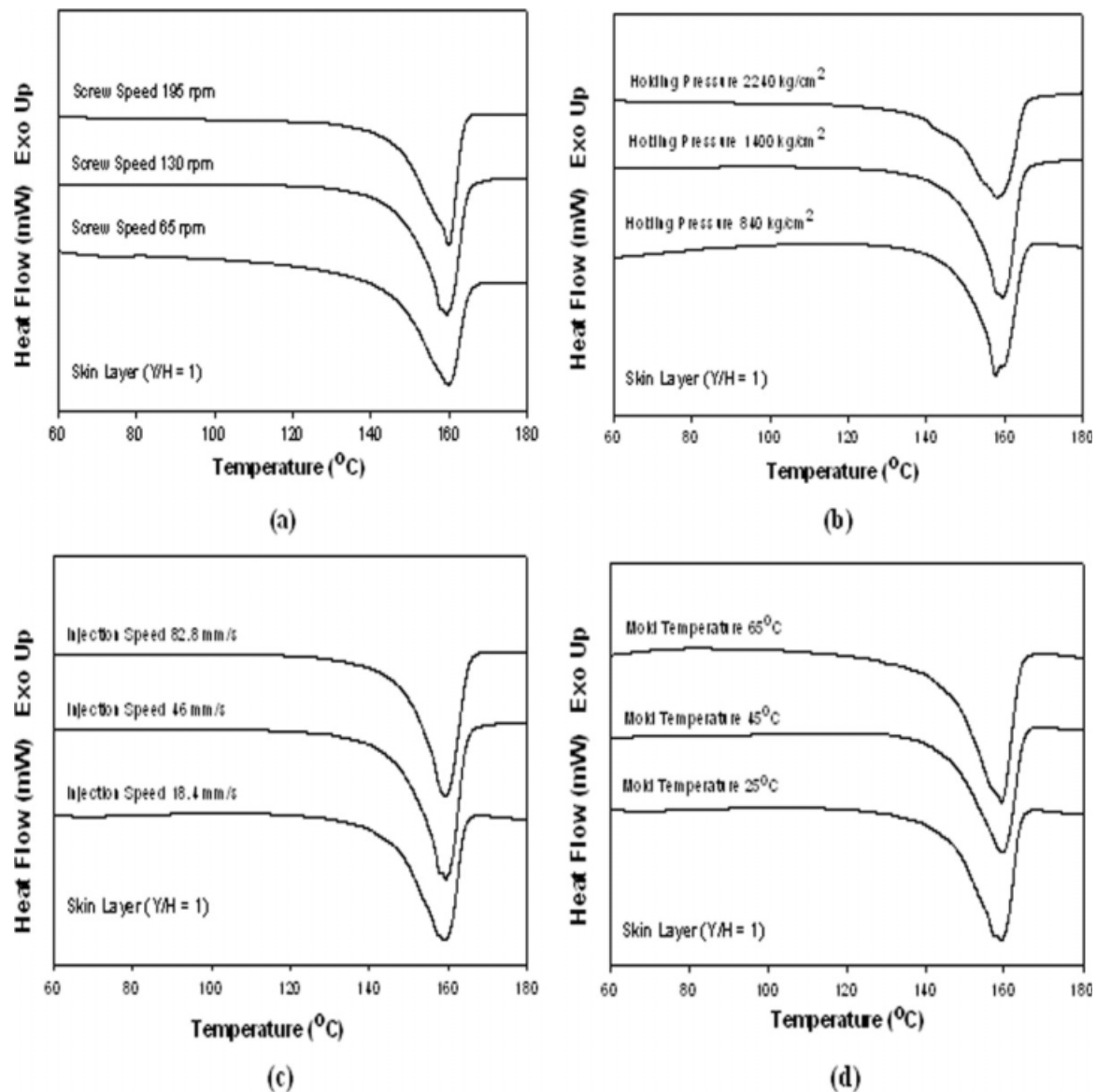


Figure 9 DSC curves of vetiver fiber-PP composites at skin layer ($Y/H = 1$) at various (a) screw speeds, (b) holding pressures, (c) injection speeds, and (d) mold temperatures.

particles were able to obstruct normal flow of polymer and impede the mobility of chain segments in melt flow more than the smaller ones.

Effect of processing conditions on PP composites

Thermal properties

As previously described in the Mechanical properties section, vetiver fiber-PP composites showed higher tensile strength and Young's modulus than that of vetiver powder-PP composites. Hence, vetiver fiber-PP composite was used to study the effect of processing conditions on properties of PP composites hereafter. DSC curves of core layer of vetiver fiber-PP composites at various screw speeds,

holding pressures, injection speeds, and mold temperatures are displayed in Figure 8(a,d), respectively. In addition, DSC curves of skin layer of vetiver fiber-PP composites at various screw speeds, holding pressures, injection speeds, and mold temperatures are illustrated in Figure 9(a,d), respectively. It was noticed that vetiver fiber-PP composites obviously exhibited more multiple and broader endotherms in the core layer than those in the skin layer. This implied that the presence of several crystallographic forms could be taken place in the core layer. However, the processing conditions had no influence on the pattern of endothermic curves and the melting range of the composites.

Gapwise crystallinity distribution at the midway of moldings of vetiver fiber-PP composites at various

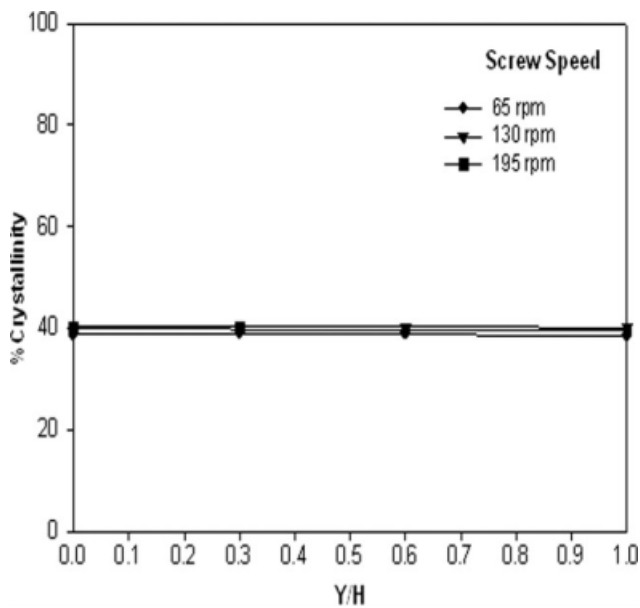


Figure 10 Gapwise crystallinity distribution at the mid-way of moldings of vetiver fiber-PP composites prepared at various screw speeds (processing condition 1, 2, and 3 according to Table I).

screw speeds, holding pressures, injection speeds, and mold temperatures are represented in Figure 10–13, respectively. It was found that screw speeds and holding pressures had no effect on degree of crystallinity of the composites. However, injection speed and mold temperature slightly affected the degree of crystallinity of the composites. Slightly higher values of degree of crystallinity were observed when injection

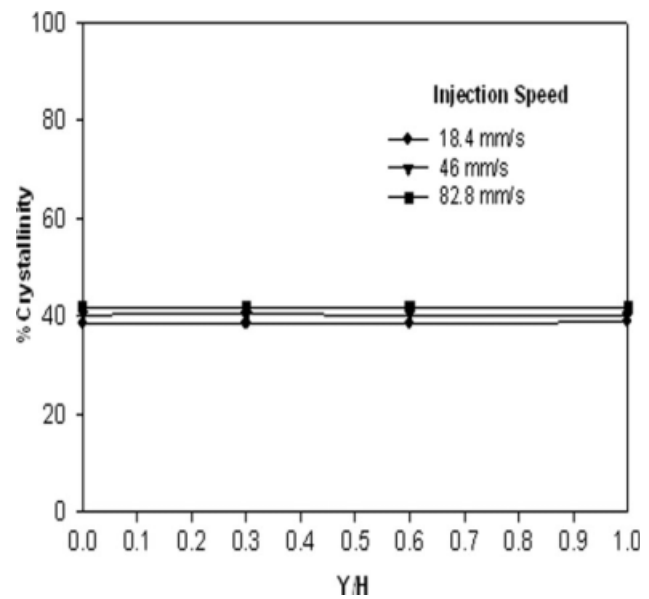


Figure 12 Gapwise crystallinity distribution at the mid-way of moldings of vetiver fiber-PP composites prepared at various injection speeds (processing condition 1, 4, and 5 according to Table I).

speeds and mold temperatures increased. This could be suggested that with increasing injection speed the melt temperature was possibly increased from the extent of shear. Hence, the polymer molecules exhibited longer relaxation time leading to an increase in degree of crystallinity of the composites. In a case of mold temperature, an increase in mold temperature led to the longer solidification time for

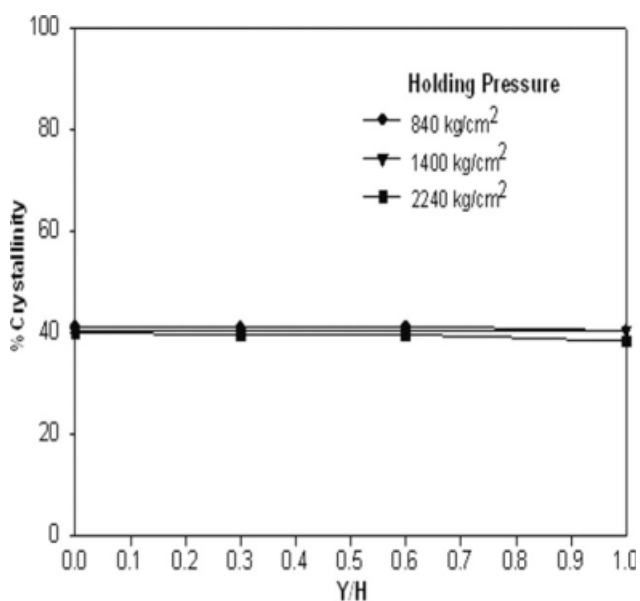


Figure 11 Gapwise crystallinity distribution at the mid-way of moldings of vetiver fiber-PP composites prepared at various holding pressures (processing condition 1, 8, and 9 according to Table I).

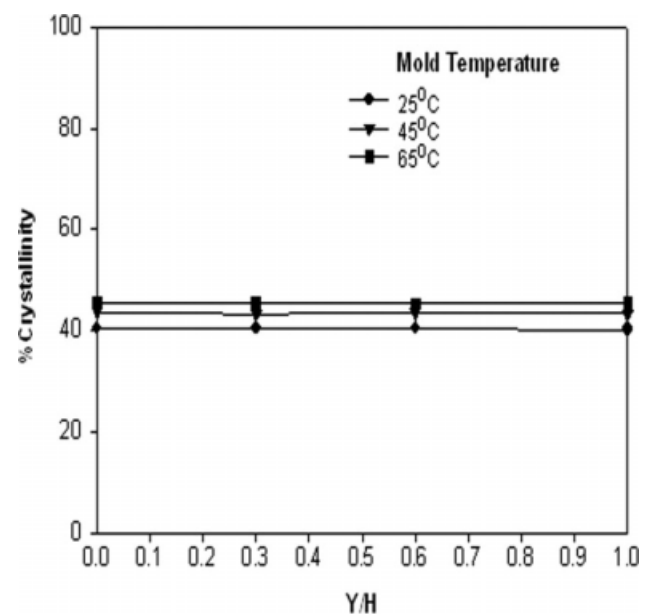


Figure 13 Gapwise crystallinity distribution at the mid-way of moldings of vetiver fiber-PP composites prepared at various mold temperatures (processing condition 4, 6, and 7 according to Table I).

TABLE IV
Mechanical Properties of Vetiver Fiber-PP Composites Prepared at Various Processing Conditions According to Table I

Processing condition	Impact strength (kJ/m ²)	Tensile strength (MPa)	Young's modulus (GPa)	Elongation at break (%)
1	18.91 ± 1.25	26.48 ± 0.54	1.43 ± 0.04	8.36 ± 0.57
2	18.58 ± 1.08	26.18 ± 0.65	1.49 ± 0.05	8.71 ± 0.97
3	18.80 ± 1.41	26.73 ± 0.58	1.44 ± 0.08	8.07 ± 0.59
4	18.19 ± 1.08	26.44 ± 0.42	1.42 ± 0.07	8.11 ± 0.41
5	17.65 ± 0.95	26.45 ± 0.42	1.38 ± 0.06	8.48 ± 0.68
6	19.20 ± 0.77	24.59 ± 0.68	1.27 ± 0.04	8.32 ± 0.43
7	21.45 ± 0.97	24.52 ± 0.53	1.16 ± 0.04	7.99 ± 0.56
8	18.80 ± 0.94	26.57 ± 0.60	1.40 ± 0.05	8.13 ± 0.56
9	18.24 ± 0.66	26.85 ± 0.43	1.35 ± 0.06	8.70 ± 0.35

polymer. As a result, degree of crystallinity of the composites increased according to an increase in relaxation time of polymer chains. This observation showed a similar result with injection molded PP studied by Li and Cheung.¹⁹ In addition, it was interesting to point out that there was no gapwise crystallinity distribution at the midway of moldings for all specimens. This phenomenon was observed in the case of PP studied by Isayev et al.⁶

Mechanical properties

Mechanical properties of vetiver fiber-PP composites prepared at various processing conditions according to Table I are summarized in Table IV. It was found that processing conditions, i.e., screw speeds, injection speeds, holding pressures, and mold temperatures, showed no significant effect on mechanical properties of vetiver fiber-PP composite. This result is in contrast with other studies on PP homopolymer. In case of PP, the processing conditions showed influences on mechanical properties.^{20,21} Fujiyama and Karger-Kocsis²⁰ reported that properties, such as flexural modulus, flexural strength, Izod impact strength, heat distortion temperature, and mold shrinkage of injection-molded PP increased as the cylinder temperature decrease because the degree of molecular orientation is higher. In addition Nagaoka et al.²¹ found that in injection molding of PP, the strengths of the specimens decreased as the mold temperature increased particularly in terms of bending properties.

The mechanical properties of the composites can be influenced by many factors, such as the matrix intrinsic properties, fiber volume fraction, and interfacial bond strength. Particularly, the interfacial bond strength between fibers and the surrounding matrix is a crucial importance for many mechanical and physical properties of composites. Hence, the interfacial bond strength between vetiver fiber and PP matrix may play an important role on the me-

chanical properties of PP composites more than the processing conditions.

Normalized thickness of shear-induced crystallization layer

The normalized thickness of shear-induced crystallization layer of both PP and vetiver fiber-PP composites slightly decreased with increasing screw speed according to Figure 14. Basically, the faster the screw rotates, the higher melt temperature is generated because the amount of shear increases. As a result, the growth of shear-induced crystallization layer could possibly minimized as observed at higher screw speed.

Furthermore, it was revealed that both normalized thickness of shear-induced crystallization layer of PP and vetiver fiber-PP composites gradually increased

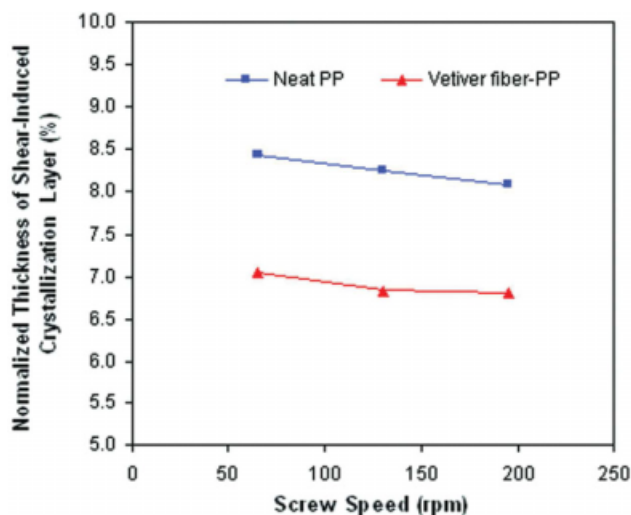


Figure 14 Normalized thickness of shear-induced crystallization layer of neat PP and vetiver fiber-PP composites prepared at various screw speeds (processing condition 1, 2, and 3 according to Table I). [Color figure can be viewed in the online issue, which is available at www.interscience.wiley.com.]

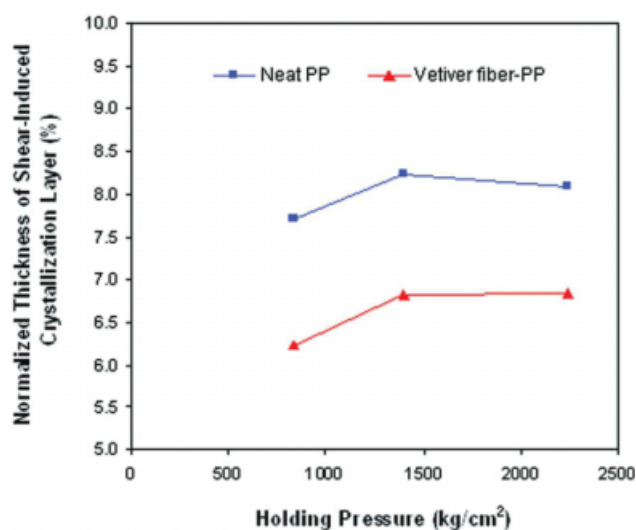


Figure 15 Normalized thickness of shear-induced crystallization layer of PP and vetiver fiber-PP composites prepared at various holding pressures (processing condition 1, 8, and 9 according to Table I). [Color figure can be viewed in the online issue, which is available at www.interscience.wiley.com.]

when holding pressure increased up to 1400 kg/cm². After that it remained unchanged (Fig. 15). An increase in holding pressure resulted in the retardation of molecular relaxation. Consequently, the shear-induced molecular orientation had no enough time to relax. This caused higher normalized thickness of shear-induced crystallization layer at higher holding pressure. Trotignon and Verdu²² also hypothesized that the holding pressure acts as a quenching phenomenon to the crystallization and perturbs relaxation of molecular chains. Furthermore, Sjönell et al.²³ reported that the holding pressure clearly affected the orientation of molecules especially in the shear zone of injection molded PP discs. The average orientation is higher further in the sample molded with increasing holding pressure while the sample molded with zero holding pressure shows a much faster relaxation of oriented chains. However, Čermák et al.²⁴ found that the holding pressure does not affect the shear-induced crystallization layer and morphology of iPP specimen.

Moreover, normalized thickness of shear-induced crystallization layer of both PP and vetiver fiber-PP composites decreased with increasing injection speed according to Figure 16. The injection speed refers to the speed of mold filling when the screw is acting as a ram. Thus, the injection speed controls the shear rate level imposed to the material during a filling stage. However, the effect of injection speed on normalized thickness of shear-induced crystallization layer was contributed from both the extent of shear (increased with increasing injection speed) and the shearing time (increased with decreasing injection

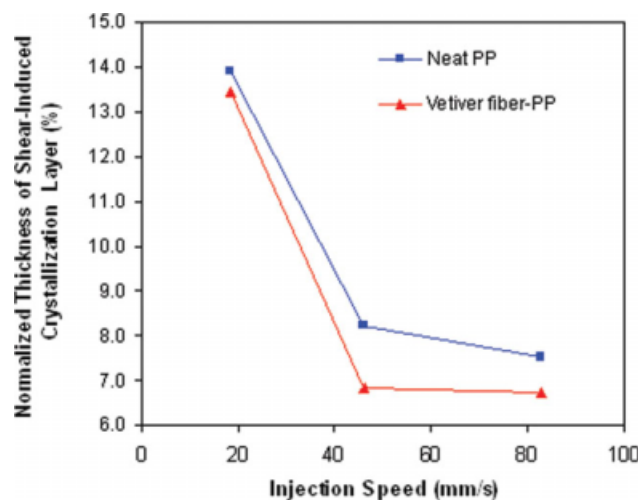


Figure 16 Normalized thickness of shear-induced crystallization layer of neat PP and vetiver fiber-PP composites prepared at various injection speeds (processing condition 1, 4, and 5 according to Table I). [Color figure can be viewed in the online issue, which is available at www.interscience.wiley.com.]

speed). In this study, it was found that the shearing time showed much more influence on the development of shear-induced crystallization layer than the extent of shear. Hence, at higher injection speed, the shearing time was lower resulting in the thinner shear-induced crystallization layer.

In addition, it was shown that the normalized thickness of shear-induced crystallization layer of both neat PP and vetiver fiber-PP composites decreased with increasing mold temperature (Fig. 17).

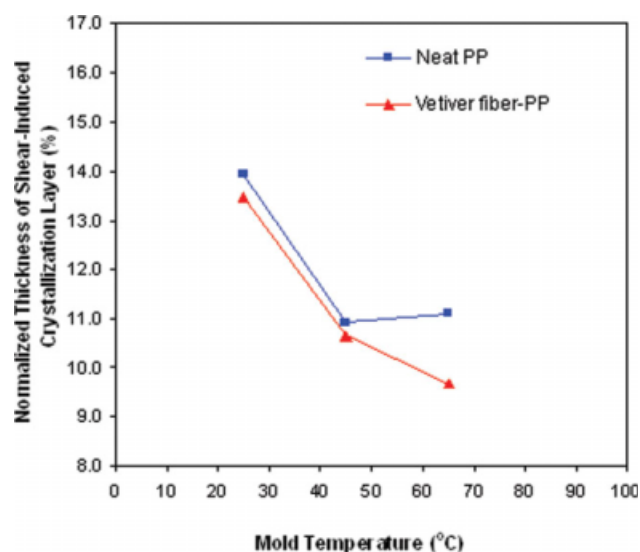


Figure 17 Normalized thickness of shear-induced crystallization layer of neat PP and vetiver fiber-PP composites prepared at various mold temperatures (processing condition 4, 6, and 7 according to Table I). [Color figure can be viewed in the online issue, which is available at www.interscience.wiley.com.]

Generally, an increase in mold temperature leads to less oriented chains due to the more possible relaxation of polymer molecule. This result showed a well agreement with Čermák et al.,²⁴ Fujiyama and Karger-Kocsis,²⁰ and Kim et al.²⁵ In comparison, vetiver fiber-PP composites showed lower normalized thickness of shear-induced crystallization layer than neat PP. This may be due to the vetiver grass acting as an obstruction to the normal flow of the melt. As a result, the molecular orientation of vetiver fiber-PP composite was less than that of PP leading to the thinner normalized thickness of shear-induced crystallization layer.

CONCLUSIONS

Alkali-treated vetiver grass exhibited higher thermal stability than that of untreated vetiver grass. DRIFT spectra and SEM micrographs of the alkali-treated vetiver grass revealed that low-molecular weight substances in vetiver grass were removed after the alkalization. Shear viscosity of both vetiver fiber-PP and vetiver powder-PP composites were higher than that of neat PP. Normalized thickness of shear-induced crystallization layer of neat PP was higher than those of vetiver fiber-PP and vetiver powder-PP composites. In addition, vetiver fiber-PP composites had higher tensile strength and higher Young's modulus than vetiver powder-PP composites. In case of the effect of processing conditions on PP composites, results indicated that injection speed and mold temperature affected the normalized thickness of shear-induced crystallization layer and degree of crystallinity of PP composites. However, processing conditions showed insignificant effect on the mechanical properties of vetiver fiber-PP composites. Moreover, it was found that the degree of crystallinity showed no distribution across the gapwise direction of the composites.

The authors thank Mettler-Toledo (Thailand) for providing DSC instrument, The Land Development Department, Nakorn Ratchasima, Thailand for supplying vetiver grass.

References

- Joshi, S. V.; Drzal, L. T.; Mohanty, A. K.; Arora, S. *Compos A* 2004, 35, 371.
- Methacanon, P.; Chaikumpollert, O.; Thavornniti, P.; Suchiva, K. *Carbohydr Polym* 2003, 54, 335.
- Chaikumpollert, O.; Methacanon, P.; Suchiva, K. *Carbohydr Polym* 2004, 57, 191.
- Ruksakulpiwat, Y.; Suppakarn, N.; Sutapun, W.; Thomthong, W. *Compos A* 2007, 38, 590.
- Somnuk, U.; Eder, G.; Phinyocheep, P.; Suppakarn, N.; Sutapun, W.; Ruksakulpiwat, Y. *J Appl Polym Sci* 2007, 106, 2997.
- Isayev, A. I.; Churdpant, Y.; Guo, X. *Intern Polym Process* 2000, 15, 72.
- Amash, A.; Zugenmaier, P. *Polymer* 2000, 41, 1589.
- van Krevelen, D. W. *Properties of Polymer*; Elsevier Science: New York, 1997.
- Ray, D.; Sakar, B. K.; Rana, A. K. *J Appl Polym Sci* 2002, 85, 2594.
- Albano, C.; González, J.; Ichazo, M.; Kaiser, D. *Polym Degrad Stab* 1999, 66, 179.
- Joseph, P. V.; Joseph, K.; Thomas, S.; Pillai, C. K. S.; Prasad, V. S.; Groeninckx, G. *Compos A* 2003, 34, 253.
- Mwaikambo, L. Y.; Ansell, M. P. *J Appl Polym Sci* 2002, 84, 2222.
- Ray, D.; Sarker, K. *J Appl Polym Sci* 2001, 80, 1013.
- Mwaikambo, L. Y.; Ansell, M. P. *Die Angew Makromo Chem* 1999, 272, 108.
- Jähn, A.; Schröder, M. W.; Fütting, M.; Schenzel, K.; Diepenbrock, W. *Spectrochim Acta Part A* 2002, 58, 2271.
- Pukánsky, B. In *Polypropylene: Structure Blends and Composites*, Vol. 3, Composites; Karger-Kocsis, J., Ed.; Chapman & Hall: London, 1995.
- Karger-Kocsis, J. In *Polypropylene: Structure Blends and Composites*, Vol. 3, Composites; Karger-Kocsis, J., Ed.; Chapman & Hall: London, 1995.
- George, J.; Thomas, S. In *Handbook of Engineering Polymeric Materials*; Cheremisinoff, N. P., Ed.; Marcel Dekker: New York, 1997.
- Li, J. X.; Cheung, W. L. *J Mater Process Tech* 1997, 63, 472.
- Fujiyama, M. *Polypropylene: Structure Blends and Composites*, Vol. 1, Structure and Morphology; Karger-Kocsis, J., Ed.; Chapman & Hall: London, 1995.
- Nagaoka, T.; Ishiaku, U. S.; Tomari, T.; Hamada, H.; Takashima, S. *Polym Test* 2005, 24, 1062.
- Trotignon, J. P.; Verdu, J. *J App Polym Sci* 1990, 39, 1215.
- Sjönell, Y.; Terselius, B.; Jansson, J.-F. *Polym Eng Sci* 1995, 35, 950.
- Čermák, R.; Obadal, M.; Ponižil, P.; Polášková, M.; Stoklasa, K.; Lengálová, A. *Euro Polym J* 2005, 41, 1838.
- Kim, K. H.; Isayev, A. I.; Kwon, K.; van Sweden, C. *Polymer* 2005, 46, 4183.